Journal of Computational and Applied Mechanics, Vol. 1., No. 2., (2000) pp. 235–258

NUMERICAL TREATMENT OF ELASTOPLASTIC PROBLEMS BY THE p-VERSION OF THE FINITE ELEMENT METHOD

István Páczelt, Frigyes Nándori
Department of Mechanics, University of Miskolc
3515 Miskolc – Egyetemváros, Hungary
mechpacz@gold.uni-miskolc.hu, mechnf@gold.uni-miskolc.hu

Tamás Szabó
Computational Mechanics Research Group, Hungarian Academy of Sciences
3515 Miskolc – Egyetemváros, Hungary
mechsza@gold.uni-miskolc.hu

[Received: September 19, 2000]

Abstract. The constitutive equations are formulated in the unrotated reference frame. Kinematic and isotropic hardening rules are assumed and the radial return mapping algorithm is applied to find the actual yield surface. By assuming large and incompressible plastic deformations, the total Lagrangian formulation of the finite element method is applied with p-extension elements making use of the truncated space and the product space.

Keywords: Elastoplastic problems, large strains, finite elements with p-extension

1. Introduction

Workstations and the latest PC-s make the numerical solution of plastic problems with large strains possible. A great number of conferences have been devoted to the problems arising during the simulation of plastic processes [1]-[9]. More and more papers are published with the aim of developing effective procedures for the solution of plastic problems. Finite rotations of material axes make the treatment of strain-stress rates and their numerical integration over a load step difficult. As is well known, there are various objective stress rates, the rules for their systematic constructions and a couple of new ones are presented in the paper [10] by Kozák.

The Jauman stress rate has been used in large strain plastic problems over the past ten years. However, stress oscillations were experienced for large rotations and during the treatment of a complex material behavior (e.g., viscoplasticity, kinematic hardening, isotropic hardening).

The oscillatory response can be removed if the Cauchy stress measure and its objective rate are defined in an unrotated orthogonal reference frame established by means of the polar decomposition of the deformation gradient at each material point. Using this concept, it can be shown that the stress response will increase monotonically in simple shear for incremental linear-elasticity. The same idea was used by Hallquist

[5,6] to work out implicit dynamic codes and by Flangan and Taylor [4] to develop codes for a transient dynamic analysis with explicit time integration. With the strains, stresses and their objective rates, each defined in the unrotated frame, the structure of small-strain plasticity is fully retained, which is advantageous to develop a finite element code. This concept firstly used by Hallquist was further developed by Healy and Dodds [7].

In this paper first we will summarize the kinematics of finite deformations, then present the strain-stress rates and the elastoplastic constitutive equations by assuming that the kinematic and isotropic hardening rules are valid. Finally, we will apply the finite element method to axisymmetric problem with p-extension elements. The approximation of the p-extension elements can be constructed either by the truncated space or the product space [18]. The two approaches are different in the number of the bubble functions. The approximations of the displacement field and the volumetric change will also be investigated. Numerical examples demonstrate the effectiveness of the applied elastoplastic theory.

2. State variables

A number of textbooks are devoted to the formulation of nonlinear solid mechanics – see for instance [2, 12]. Here we summarize the most important basic relations that are required for a finite element formulation.

In our analysis we consider the motion of a body in a fixed Cartesian coordinate system $(X_1,\ X_2,\ X_3)$. The position vector of a generic material point is denoted by $\mathbf{X}$ at time 0 (in the reference or undeformed configuration), and by $\mathbf{x}$ at time t (in the deformed or current configuration). The reference and deformed configurations are denoted by B_0 and B, respectively.

The displacement vector is given by

$$\mathbf{u} = \mathbf{x} - \mathbf{X} \,. \tag{2.1}$$

The fundamental measure of deformation is the deformation gradient

$$\mathbf{F} = \frac{\partial \mathbf{x}}{\partial \mathbf{X}} \,. \tag{2.2}$$

If the mapping $\mathbf{X} = \mathbf{x}(\mathbf{X}, t)$ is one-to-one, then

$$J = \det \mathbf{F} > 0 \,. \tag{2.3}$$

As is well known, the deformation gradient $\mathbf{F}$ can be decomposed into a product of two matrices

$$\mathbf{F} = \mathbf{V} \cdot \mathbf{R} = \mathbf{R} \cdot \mathbf{U} \tag{2.4}$$

where $\mathbf{R}$ is the orthogonal rotation tensor, while $\mathbf{V}$ and $\mathbf{U}$ are the symmetric left and right stretch tensors. The principal values λ_i of $\mathbf{V}$ and $\mathbf{U}$ are equal.

The velocity field, which is the material time derivative of the displacements, is written as

$$\mathbf{v} = \frac{\partial \mathbf{x}}{\partial t} = \dot{\mathbf{x}}\,. \tag{2.5}$$

The velocity gradient $\mathbf{L}$ (velocity strain tensor) is defined as the gradient of the velocity field with respect to the current configuration. Making use of the chain rule and (2.2), we can write

$$\mathbf{L} = \frac{\partial \mathbf{v}}{\partial \mathbf{x}} = \frac{\partial \mathbf{v}}{\partial \mathbf{X}}\frac{\partial \mathbf{X}}{\partial \mathbf{x}} = \dot{\mathbf{F}} \cdot \mathbf{F}^{-1}\,. \tag{2.6}$$

We denote the symmetric and skew parts of the velocity gradient by $\mathbf{D}$ (the rate of the deformation tensor) and $\mathbf{W}$ (the spin rate of the velocity gradient). According to the decomposition theorem

$$\mathbf{L} = \mathbf{D} + \mathbf{W} \qquad \text{where} \qquad \mathbf{D} = \frac{1}{2}\left(\mathbf{L} + \mathbf{L}^T\right) \qquad \text{and} \qquad \mathbf{W} = \frac{1}{2}\left(\mathbf{L} - \mathbf{L}^T\right)\,. \tag{2.7}$$

The tensors $\mathbf{D}$ and $\mathbf{W}$ are both instantaneous rates, i.e., are not associated with the load history. When integrated over the load history, the principal values of $\mathbf{D}$ are the logarithmic strains of the line elements oriented in the principal directions if the principal directions do not rotate.

Applying the polar decomposition theorem to $\mathbf{F}$, we have

$$\mathbf{L} = (\mathbf{R}\cdot\mathbf{U})^{\cdot}\cdot\mathbf{F}^{-1} = \dot{\mathbf{R}}\cdot\mathbf{U}\cdot\mathbf{F}^{-1} + \mathbf{R}\cdot\dot{\mathbf{U}}\cdot\mathbf{F}^{-1} = \\ = \dot{\mathbf{R}}\cdot\mathbf{U}\cdot\mathbf{U}^{-1}\cdot\mathbf{R}^{-1} + \mathbf{R}\cdot\dot{\mathbf{U}}\cdot\mathbf{U}^{-1}\cdot\mathbf{R}^{-1}\,,$$

since

$$(\mathbf{R}\cdot\mathbf{U})^{-1} = \mathbf{U}^{-1}\cdot\mathbf{R}^{-1} = \mathbf{U}^{-1}\mathbf{R}^T, \qquad \text{and} \qquad \boldsymbol{\Omega} = \dot{\mathbf{R}}\cdot\mathbf{R}^T\,.$$

In view of the fact that $\mathbf{R}$ is an orthogonal tensor ($\mathbf{R}^T = \mathbf{R}^{-1}$) we obtain

$$\mathbf{L} = \dot{\mathbf{R}}\mathbf{R}^T + \mathbf{R}\cdot\dot{\mathbf{U}}\cdot\mathbf{U}^{-1}\cdot\mathbf{R}^T = \boldsymbol{\Omega} + \mathbf{R}\cdot\dot{\mathbf{U}}\cdot\mathbf{U}^{-1}\cdot\mathbf{R}^T\,. \tag{2.8}$$

Furthermore, we have

$$\mathbf{R}^T\cdot\mathbf{R} = \mathbf{1} \qquad \text{and} \qquad \frac{d\left(\mathbf{R}^T\mathbf{R}\right)}{dt} = \mathbf{0}$$

in which $\mathbf{1}$ is the unit tensor. It is obvious that

$$\dot{\mathbf{R}}^T\cdot\mathbf{R} = -\mathbf{R}^T\cdot\dot{\mathbf{R}}\,. \tag{2.9}$$

With (2.8), $(2.7)_2$ yields

$$\mathbf{D} = \mathbf{R}\cdot\frac{1}{2}\left(\dot{\mathbf{U}}\cdot\mathbf{U}^{-1} + \mathbf{U}^{-1}\cdot\dot{\mathbf{U}}\right)\cdot\mathbf{R}^T \equiv \mathbf{R}\cdot\mathbf{d}\cdot\mathbf{R}^T \tag{2.10a}$$

where $\mathbf{d}$ is the unrotated deformation rate:

$$\mathbf{d} = \frac{1}{2}\left(\dot{\mathbf{U}}\cdot\mathbf{U}^{-1} + \mathbf{U}^{-1}\cdot\dot{\mathbf{U}}\right) = \mathbf{R}^T\mathbf{D}\mathbf{R}\,. \tag{2.10b}$$

The double scalar product of the Cauchy stress tensor $\mathbf{T}$ and the rate of deformation tensor $\mathbf{D}$ gives the stress power per unit volume

$$\mathbf{T} : \mathbf{D} \,. \tag{2.11}$$

Introducing the unrotated Cauchy stress tensor

$$\mathbf{t} = \mathbf{R}^T \cdot \mathbf{T} \cdot \mathbf{R} \,, \tag{2.12}$$

the double scalar product (2.11) can be written as

$$\mathbf{T} : \mathbf{D} = \mathbf{R}^T \cdot \mathbf{T} \cdot \mathbf{R} : \mathbf{R}^T \cdot \mathbf{D} \cdot \mathbf{R} = \mathbf{t} : \mathbf{d} \,. \tag{2.13}$$

The right and left Cauchy-Green tensors $\mathbf{C}$ and $\mathbf{D}$ are defined by

$$\mathbf{C} = \mathbf{F}^T \cdot \mathbf{F} = \mathbf{U}^2 \qquad \text{and} \qquad \mathbf{B} = \mathbf{F} \cdot \mathbf{F}^T = \mathbf{V}^2 \,, \tag{2.14}$$

respectively. We remark that the eigenvalues of the two tensors are identical but the eigenvectors are different.

We adopt the total Lagrangian formulation of the problem. This means that all quantities are taken in the reference configuration. As is well known, the deformation measure, i.e., the Green-Lagrange strain tensor is defined by

$$\mathbf{E} = \frac{1}{2} \left(\mathbf{U}^2 - \mathbf{1} \right) = \frac{1}{2} \left(\mathbf{F}^T \cdot \mathbf{F} - \mathbf{1} \right) \,. \tag{2.15}$$

Furthermore, we have

$$\dot{\mathbf{E}} = \frac{1}{2} \left(\dot{\mathbf{F}}^T \cdot \mathbf{F} + \mathbf{F}^T \cdot \dot{\mathbf{F}} \right) = \mathbf{F}^T \cdot \mathbf{D} \cdot \mathbf{F} \,, \tag{2.16}$$

which, as can be seen by using (2.6) and (2.7), includes the velocity gradient

$$\mathbf{D} = \frac{1}{2} \left(\dot{\mathbf{F}} \cdot \mathbf{F}^{-1} + \left(\mathbf{F}^{-1} \right)^T \cdot \dot{\mathbf{F}}^T \right) \,.$$

Substituting the polar decomposition $\mathbf{F} = \mathbf{R} \cdot \mathbf{U}$ into equation (2.16), we obtain

$$\dot{\mathbf{E}} = \mathbf{U}^T \cdot \mathbf{R}^T \cdot \mathbf{D} \cdot \mathbf{R} \cdot \mathbf{U} \tag{2.17}$$

from which, with regard to equation (2.10b), it follows

$$\dot{\mathbf{E}} = \mathbf{U}^T \cdot \mathbf{d} \cdot \mathbf{U} \,. \tag{2.18}$$

Since $\mathbf{U} = \mathbf{U}^T$ is a symmetric tensor, the unrotated deformation rate $\mathbf{d}$ can be expressed from (2.18):

$$\mathbf{d} = \mathbf{U}^{-1} \cdot \dot{\mathbf{E}} \cdot \mathbf{U}^{-1} \,. \tag{2.19}$$

The work-conjugate of the Green-Lagrange strain tensor $\mathbf{E}$ is the second Piola-Kirchhoff stress tensor $\mathbf{P}^{II}$, which can be given in terms of the Cauchy stress tensor $\mathbf{T}$ as follows

$$\mathbf{P}^{II} = J \, \mathbf{F}^{-1} \cdot \mathbf{T} \cdot \mathbf{F}^{-T} \,. \tag{2.20}$$

Substituting the polar decomposition $\mathbf{F} = \mathbf{R} \cdot \mathbf{U}$ into (2.20) and using (2.12), we have

$$\mathbf{P}^{II} = J\,\mathbf{U}^{-1} \cdot \mathbf{t} \cdot \mathbf{U}^{-1}\,. \tag{2.21}$$

Deriving this equation with respect to time t, we obtain a formula for the rate of the stress tensor

$$\dot{\mathbf{P}}^{II} = \dot{J}\,\mathbf{U}^{-1} \cdot \mathbf{t} \cdot \mathbf{U}^{-1} + J\,\left(\mathbf{U}^{-1}\right)^{\cdot} \cdot \mathbf{t} \cdot \mathbf{U}^{-1} + J\,\mathbf{U}^{-1} \cdot \dot{\mathbf{t}} \cdot \mathbf{U}^{-1} + J\,\mathbf{U}^{-1} \cdot \mathbf{t} \cdot \left(\mathbf{U}^{-1}\right)^{\cdot} \tag{2.22}$$

where

$$\dot{J} = J\,\mathrm{tr}\,(\mathbf{D}) \tag{2.23}$$

in which $\mathrm{tr}\,(\mathbf{D})$ is the trace of the tensor $\mathbf{D}$. In order to determine $(\mathbf{U}^{-1})^{\cdot}$ we consider the equation

$$\mathbf{U}^{-1} \cdot \mathbf{U} = \mathbf{1} \tag{2.24}$$

as our point of departure. Taking its derivative with respect to time t, we have

$$(\mathbf{U}^{-1})^{\cdot} \cdot \mathbf{U} + \mathbf{U}^{-1} \cdot \dot{\mathbf{U}} = \mathbf{0} \tag{2.25}$$

from which

$$(\mathbf{U}^{-1})^{\cdot} = -\mathbf{U}^{-1} \cdot \dot{\mathbf{U}} \cdot \mathbf{U}^{-1}\,. \tag{2.26}$$

Substituting (2.23) and (2.26) into (2.22) and making use of (2.21), we obtain the relation

$$\dot{\mathbf{P}}^{II} = J\,\mathbf{U}^{-1} \cdot \dot{\mathbf{t}} \cdot \mathbf{U}^{-1} + tr\,(\mathbf{D})\,\mathbf{P}^{II} - \mathbf{U}^{-1} \cdot \dot{\mathbf{U}} \cdot \mathbf{P}^{II} - \mathbf{P}^{II} \cdot \dot{\mathbf{U}} \cdot \mathbf{U}^{-1} \tag{2.27}$$

for the stress rate.

3. Large strain elastoplasticity

3.1. An objective time derivative of the Cauchy stress tensor. The constitutive law for an elastoplastic material determines the relation between a materially objective stress rate and a work conjugate deformation rate.

Let us consider the equation relating the unrotated stress tensor $\mathbf{t}$ to the Cauchy stress tensor $\mathbf{T}$:

$$\mathbf{t} = \mathbf{R}^T \cdot \mathbf{T} \cdot \mathbf{R}\,. \tag{3.1}$$

After taking the time derivative of the above equation, we get

$$\dot{\mathbf{t}} = \dot{\mathbf{R}}^T \cdot \mathbf{T} \cdot \mathbf{R} + \mathbf{R}^T \cdot \dot{\mathbf{T}} \cdot \mathbf{R} + \mathbf{R}^T \cdot \mathbf{T} \cdot \dot{\mathbf{R}}\,. \tag{3.2}$$

Utilizing the expression $\boldsymbol{\Omega} = \dot{\mathbf{R}} \cdot \mathbf{R}^T$ in (2.8), we can express the rate of the orthogonal rotation tensor and its transpose:

$$\dot{\mathbf{R}} = \boldsymbol{\Omega} \cdot \mathbf{R}\,, \qquad \dot{\mathbf{R}}^T = \mathbf{R}^{\mathbf{T}} \cdot \boldsymbol{\Omega}^T = -\mathbf{R}^T \cdot \boldsymbol{\Omega} \tag{3.3}$$

by which equation (3.2) gives

$$\dot{\mathbf{t}} = \mathbf{R}^T \cdot \mathbf{T}^{\nabla} \cdot \mathbf{R}, \qquad \mathbf{T}^{\nabla} = \dot{\mathbf{T}} - \boldsymbol{\Omega} \cdot \mathbf{T} + \mathbf{T} \cdot \boldsymbol{\Omega} \tag{3.4}$$

where $\mathbf{T}^{\nabla}$ is the Green-Naghdi objective stress rate tensor [2, 10].

With the tensor of material constants $\mathbf{C}^{ep}$ the constitutive equation takes the form

$$\mathbf{T}^{\nabla} = \mathbf{C}^{ep} \colon \mathbf{D} \,. \tag{3.5}$$

Let us reformulate the constitutive law in the unrotated but deformed configuration. Making use of equations (3.4), (3.5) and (2.10b), we have

$$\dot{\mathbf{t}} = \mathbf{R}^T \cdot (\mathbf{C}^{ep} : \mathbf{D}) \cdot \mathbf{R} = \mathbf{C}^{ep} : (\mathbf{R}^T \cdot \mathbf{D} \cdot \mathbf{R}) = \mathbf{C}^{ep} : \mathbf{d} \,. \tag{3.6}$$

One can see from equation (3.6) that the integration of the rate of the rotation tensor over the load history is avoided. However, all quantities should be transformed into the unrotated deformed configuration. Constitutive law (3.6) was first used by Hallquist [5]. When this method is chosen it is essential to perform the polar decomposition of the deformation gradient as accurately as possible.

3.2. Determination of the elastoplastic state. We shall assume that the material is isotropic and the undeformed configuration is stress free. The Mises yield surface is applied together with the associated flow rule. The hardening rule, which specifies how the yield function is modified during a plastic flow, can be kinematic, isotropic or a combination of the previous two. The yield surface is given as

$$f\ (\boldsymbol{\xi}, \overline{e}^p) = \|\boldsymbol{\xi}\| - \sqrt{\frac{2}{3}}\ \ (\overline{e}^p) \leq 0 \tag{3.7}$$

where

- $(\overline{e}^p)$ is the hardening rule,
- $\boldsymbol{\xi} = \mathbf{s} - \boldsymbol{\alpha}$, in which the deviatoric stress $\mathbf{s} = \operatorname{dev} \mathbf{t} = \mathbf{t} - \frac{1}{3} tr\,(\mathbf{t})\,\mathbf{1}$, $\boldsymbol{\alpha}$ is the centre of the yield surface (called back stress),
- $\|\boldsymbol{\xi}\| = \sqrt{\boldsymbol{\xi} : \boldsymbol{\xi}}$,
- $\overline{e}^p$ is the equivalent plastic strain $\overline{e}^p = \int\limits_0^t \sqrt{\frac{2}{3}}\, \|\mathbf{d}^p\,(\tau)\|\, d\tau$,
- $\mathbf{d} = \mathbf{d}^e + \mathbf{d}^p$ is the strain rate decomposed into elastic and plastic parts.

The decomposition of $\mathbf{d}$ is based on the decomposition of the deformation gradient proposed by Lee [11] for ductile metals

$$\mathbf{F} = \mathbf{F}^e \cdot \mathbf{F}^p \tag{3.8}$$

where $\mathbf{F}^e$ represents the elastic deformation, i.e., the distortion of the lattice, while $\mathbf{F}^p$ represents the plastic deformation. Substituting (3.8) into (2.6), we have

$$\mathbf{L} = \dot{\mathbf{F}} \cdot \mathbf{F}^{-1} = \dot{\mathbf{F}}^e \cdot \mathbf{F}^p \cdot \left(\mathbf{F}^{-p} \cdot \mathbf{F}^{-e}\right) + \mathbf{F}^e \cdot \dot{\mathbf{F}}^p \cdot \left(\mathbf{F}^{-p} \cdot \mathbf{F}^{-e}\right) =$$
$$= \dot{\mathbf{F}}^e \cdot \mathbf{F}^{-e} + \mathbf{F}^e \cdot \dot{\mathbf{F}}^p \cdot \mathbf{F}^{-p} \cdot \mathbf{F}^{-e} \equiv \mathbf{L}^e + \mathbf{F}^e \cdot \mathbf{L}^p \cdot \mathbf{F}^{-e} \tag{3.9}$$

We shall assume in the course of elastoplastic deformations that the elastic strains are vanishingly smaller than the plastic strains. Furthermore, we shall also assume for the elastic deformation that $\mathbf{F}^e = \mathbf{V}^e$ in (3.9), i.e., the rigid rotation is added to plastic term. Hence, we can rewrite the decomposition

$$\mathbf{F} = \mathbf{F}^e \cdot \mathbf{F}^p = \mathbf{V}^e \cdot \mathbf{V}^p \cdot \mathbf{R}. \tag{3.10}$$

Assuming small elastic strains $\boldsymbol{\varepsilon}^e$, it holds

$$\mathbf{F}^e = \mathbf{1} + \boldsymbol{\varepsilon}^e \approx \mathbf{1}\,. \tag{3.11}$$

Consequently, we can decompose the approximation of the velocity strain tensor and its symmetric part into the forms

$$\mathbf{L} \approx \mathbf{L}^e + \mathbf{L}^p, \qquad \text{and} \qquad \mathbf{D} \approx \mathbf{D}^e + \mathbf{D}^p. \tag{3.12}$$

Substituting $(3.12)_2$ into (2.10b) the unrotated deformation rate can also be decomposed into elastic and plastic parts

$$\mathbf{d} = \mathbf{R}^T \cdot (\mathbf{D}^e + \mathbf{D}^p) \cdot \mathbf{R} = \mathbf{d}^e + \mathbf{d}^p \tag{3.13}$$

as is the case for small strain plasticity.

3.3. Determination of the stresses in the unrotated configuration. The integration of the plastic equations is performed over finite time increments. A good review can be found in the works of Simo and Taylor [16,17]. The radial return mapping procedure seems to be very effective for integrating the elastoplastic problem numerically.

Imposing kinematic and isotropic hardening rules, the yield surface will be both translated and inflated. The translation is associated with the plastic modulus $H'_\alpha\,(\overline{e}^p)$, and the inflation with the hardening rule $\quad(\overline{e}^p)$, where e is the equivalent strain.

Points inside the yield surface (3.7) ($f \leq 0$) refer to elastic states, and points on the yield surface ($f = 0$) refer to plastic states.

As is known from the Prandtl-Reuss equations

$$\mathbf{s} = 2G(\dot{\mathbf{e}} - \dot{\mathbf{e}}^p)\,, \tag{3.14}$$

where $\mathbf{s}$ is the deviatoric stress rate, $\dot{\mathbf{e}}$ is the deviatoric strain rate, $\dot{\mathbf{e}}^p$ is the plastic part of the deviatoric strain rate, G is the elastic shear modulus and

$$\mathbf{e} = \boldsymbol{\varepsilon} - \frac{1}{3}\mathrm{tr}\,(\boldsymbol{\varepsilon})\,\mathbf{1} \tag{3.15}$$

where $\boldsymbol{\varepsilon}$ is the strain tensor. According to the associative rule

$$\mathbf{d}^p = \dot{\mathbf{e}}^p = \gamma \frac{\partial f}{\partial \boldsymbol{\xi}} = \gamma \hat{\mathbf{n}} \tag{3.16a}$$

where γ is the plastic coefficient:

$$\gamma \equiv \|\dot{\mathbf{e}}^p\| = \left\| \gamma \frac{\partial f}{\partial \boldsymbol{\xi}} \right\| = \|\gamma \hat{\mathbf{n}}\| = \frac{1}{1 + \frac{{}'+H'_\alpha}{3G}}\,. \tag{3.16b}$$

Here $H_{\alpha}^{'}(\overline{e}^{p})$ and $'(\overline{e}^{p})$ are obtained by derivation with respect to $\overline{e}^{p}$ and $\hat{\mathbf{n}}$ is the unit normal of the yield surface:

$$\hat{\mathbf{n}} = \frac{\boldsymbol{\xi}}{\|\boldsymbol{\xi}\|} \ . \tag{3.16c}$$

The translation rate of the centre of the yield surface is given by

$$\dot{\boldsymbol{\alpha}} = \frac{2}{3} H_{\alpha}^{'}(\overline{e}^{p})\, \dot{\mathbf{e}}^{p} \tag{3.17}$$

where $H_{\alpha}^{'}(\overline{e}^{p})$ is the plastic modulus.

The pressure rate due to the elastic volume change is calculated as

$$\dot{p} = \frac{1}{2}\mathrm{tr}\,(\dot{\mathbf{t}}) = K\,\mathrm{tr}\,(\dot{\boldsymbol{\varepsilon}}) \tag{3.18}$$

where K is the bulk modulus: $K = E/(3-6\nu)$, E is the Young's modulus, ν is the Poisson's ratio.

Regarding equation (3.14) as our point of departure, a standard transformation leads to the following equation

$$\dot{\mathbf{s}} = 2G[\mathbf{I} - \gamma\hat{\mathbf{n}} \otimes \hat{\mathbf{n}}] : \dot{\mathbf{e}} \tag{3.19}$$

in which $\mathbf{I}$ is a fourth order unit tensor, $\otimes$ denotes the tensor product, the element $ijkl$ of the tensor $[\hat{\mathbf{n}} \otimes \hat{\mathbf{n}}]$ is evaluated from the relation $\hat{n}_{ij}\hat{n}_{kl}$, and $\hat{n}_{ij}$ is the element of the tensor $\hat{\mathbf{n}}$.

In view of the representation

$$\mathbf{t} = \mathbf{s} + \frac{1}{3}\mathrm{tr}\,(\mathbf{t})\,\mathbf{1}\ , \tag{3.20}$$

a rate constitutive equation can be obtained by using (3.15), (3.18) and (3.19):

$$\dot{\mathbf{t}} = \mathbf{C}^{ep}(\mathbf{t}) : \dot{\boldsymbol{\varepsilon}} \tag{3.21}$$

where $\mathbf{C}^{ep}$ is the fourth order tensor of the tangent moduli

$$\mathbf{C}^{ep}(\mathbf{t}) = K\,\mathbf{1} \otimes \mathbf{1} + 2G\left[\mathbf{I} - \frac{1}{3}\mathbf{1} \otimes \mathbf{1}\right] - 2G\gamma\hat{\mathbf{n}} \otimes \hat{\mathbf{n}} \quad . \tag{3.22}$$

Integration of the nonlinear equation (3.19) with respect to time t is not simple since the elastoplastic problem depends on the load history. A great number of return mapping algorithms are available. The radial return mapping seems to be the most efficient procedure (see Appendix 1).

4. Consistent tangential stiffness matrix

With the knowledge of $\boldsymbol{\sigma}_n$, $\overline{e}_n^{p}$ and $\boldsymbol{\varepsilon}_n$ at time t^n, the vector of the strain increments

$$\Delta\boldsymbol{\varepsilon} = \boldsymbol{\varepsilon} - \boldsymbol{\varepsilon}_n \tag{4.1}$$

can be determined by using the nonlinear constitutive law and satisfying the yield surface as well:

$$\Delta\boldsymbol{\varepsilon} \rightarrow \widetilde{\boldsymbol{\sigma}}(\mathbf{t}, \overline{e}_n^p, \boldsymbol{\varepsilon}_n, \Delta\boldsymbol{\varepsilon})\,. \tag{4.2}$$

The principle of the virtual work can be applied to find a unique value for $\Delta\boldsymbol{\varepsilon}$. The principle itself assumes the form

$$G(\mathbf{u}, \delta\mathbf{u}) = \int_V \rho\ddot{\mathbf{u}} \cdot \delta\mathbf{u}\,\mathrm{d}V + \int_V \tilde{\boldsymbol{\sigma}}\left(\mathbf{t}_n, \boldsymbol{\varepsilon}_n, \bar{e}_n^p, \nabla\mathbf{u} - \boldsymbol{\varepsilon}_n\right) : \nabla\delta\mathbf{u}\,\mathrm{d}V - \\ - \int_V \rho\mathbf{k} \cdot \delta\mathbf{u}\,\mathrm{d}V - \int_{A_p} \overline{\mathbf{p}} \cdot \delta\mathbf{u}\,\mathrm{d}A = 0 \tag{4.3}$$

where $\delta\mathbf{u}$ is the variation of $\mathbf{u}$ ($\delta\mathbf{u} = \mathbf{0}$ if $\mathbf{r} \in A_u$), $\rho\mathbf{k}$ stands for the body forces and $\ddot{\mathbf{u}}$ is the acceleration.

Equation (4.3) can be written in linearized form and can be solved with the Newton iteration. This means that one should solve a sequence of linearized problems given by

$$DG(\mathbf{u}_{n+1}^{(i)}, \delta\mathbf{u}) \cdot \Delta\mathbf{u}_{n+1}^{(i)} \equiv \int_V \nabla\delta\mathbf{u} : \left[\mathbf{C}_{n+1}^{(i)} : \nabla\left(\Delta\mathbf{u}_{n+1}^{(i)}\right)\right]\,\mathrm{d}V = -G(\mathbf{u}_{n+1}^{(i)}, \delta\mathbf{u}) \tag{4.4}$$

until the residual $G(\mathbf{u}_{n+1}^{(i)}, \delta\mathbf{u})$ vanishes.

In order to achieve fast convergency during the numerical computations we need a constitutive tensor $\mathbf{C}_{n+1}^{(i)}$ in a consistent form. Simo and Taylor [16] gave this tensor in the following form

$$\mathbf{C}_{n+1}^{(i)} = \mathbf{C}_{n+1}^{ep} = K\,\mathbf{1}\otimes\mathbf{1} + 2G\beta\left[\mathbf{I} - \frac{1}{3}\mathbf{1}\otimes\mathbf{1}\right] - 2G\,\bar{\gamma}\,\hat{\mathbf{n}}\otimes\hat{\mathbf{n}} \tag{4.5}$$

where

$$\beta = \sqrt{\frac{2}{3}}\frac{[\ _{n+1} + \Delta H_\alpha]}{\left\|\boldsymbol{\xi}_{n+1}^*\right\|} \qquad \text{and} \qquad \bar{\gamma} = \frac{1}{1 + \frac{[\ '+\Delta H'_\alpha]_{n+1}}{3G}} - (1-\beta)\,.$$

The matrix version of (4.5), which is applied in the finite element applications, was given by Dodds [3]. This matrix relates the increments of the unrotated stresses and strains

$$\Delta\mathbf{t} = \mathbf{C}^{*ep}\Delta\mathbf{d} \tag{4.6}$$

where

$$\mathbf{C}^{*ep} = \tilde{\mathbf{C}} - 2G\gamma\,\mathbf{n}\,\mathbf{n}^T$$

($\Delta\mathbf{t}$, $\Delta\mathbf{d}, \mathbf{n}$ are vectors with six components). The components of the tensor $\tilde{\mathbf{C}}$ are as follows

$$\tilde{C}_{11} = \tilde{C}_{22} = \tilde{C}_{33} = K + \frac{4}{3}G\,\tilde{\beta}\,, \qquad \tilde{C}_{21} = \tilde{C}_{31} = \tilde{C}_{32} = K - \frac{2}{3}G\,\tilde{\beta}$$
$$\tilde{C}_{44} = \tilde{C}_{55} = \tilde{C}_{66} = G\,\tilde{\beta}\,.$$

Here

$$\tilde{\beta} = \begin{bmatrix} \mathbf{s}_{n+1}^{(i)} \colon \mathbf{s}_{n+1}^{(i)} \\ \mathbf{s}_{n+1}^{*(i)} \colon \mathbf{s}_{n+1}^{*(i)} \end{bmatrix}, \qquad \mathbf{n} = \frac{\mathbf{s}_{n+1}^{(i)}(\text{vector})}{R_{n+1}^{(i)}} \qquad \text{and} \qquad R_{n+1}^{(i)} = \sqrt{\frac{2}{3}} \left(\overline{e}_{n+1}^{p(i)}\right).$$

For the numerical treatment of large plastic deformations we shall apply the total Lagrangian formulation. The increment of the stress tensor is measured by the second Piola-Kirchhoff stress tensor $\mathbf{P}^{II}$. Using the components of stress tensor $\mathbf{P}^{II}$ we construct the vector of stresses $\mathbf{S}$ which is related to the vector of the Green-Lagrange strains $\boldsymbol{\varepsilon}_G$ through the matrix of tangent moduli. For the vectors of stresses and strain increments, we assume that

$$\mathbf{P}^{II} \quad \rightarrow \quad \Delta\mathbf{S} = \mathbf{C}^{ep}\Delta\boldsymbol{\varepsilon}_G. \tag{4.7}$$

Integrating equation (2.27) in a finite time interval, we have

$$\Delta\mathbf{P}^{II} = J\,\mathbf{U}^{-1}\cdot\Delta\mathbf{t}\cdot\mathbf{U}^{-1} + \operatorname{tr}(\Delta\mathbf{D})\,\mathbf{P}^{II} - \mathbf{U}^{-1}\cdot\Delta\mathbf{U}\cdot\mathbf{P}^{II} - \mathbf{P}^{II}\cdot\Delta\mathbf{U}\cdot\mathbf{U}^{-1}. \tag{4.8}$$

The integration of equation (2.19) gives the increment in terms of the unrotated deformation rate

$$\Delta\mathbf{d} = \mathbf{U}^{-1}\cdot\Delta\mathbf{E}\cdot\mathbf{U}^{-1}. \tag{4.9}$$

In order to obtain a symmetric matrix $\mathbf{C}^{ep}$ for the tangent moduli from the combination of (4.8), (4.9) and (4.6), we shall assume the followings:

1. Since the plastic deformation is incompressible the larger deformations are the more negligible the value of $\operatorname{tr}(\Delta\mathbf{D})$ is.
2. The term $\Delta\mathbf{U}$ is negligible comparing to $\mathbf{U}^{-1}$ and $\mathbf{P}^{II}$. This assumption will slow down the convergency to some extent.

Based on the preceding assumptions, we can write

$$\Delta\mathbf{P}^{II} = J\,\mathbf{U}^{-1}\cdot\Delta\mathbf{t}\cdot\mathbf{U}^{-1} \quad \Longrightarrow \quad \Delta\mathbf{S} = \mathbf{C}^{ep}\Delta\boldsymbol{\varepsilon}_G \tag{4.10}$$

where

$$\mathbf{C}^{ep} = J\mathbf{Q}\mathbf{C}^{*ep}\mathbf{Q}^T. \tag{4.11}$$

Making use of the notations

$$u_1 = U_{11}^{-1}, \quad u_2 = U_{21}^{-1}, \quad u_3 = U_{22}^{-1}, \quad u_4 = U_{31}^{-1}, \quad u_5 = U_{32}^{-1}, \quad u_6 = U_{33}^{-1},$$

the matrix $\mathbf{Q}$ can be given in the form

$$\mathbf{Q} = \begin{bmatrix} u_1^2 & u_2^2 & u_4^2 & 2u_1u_2 & 2u_2u_4 & 2u_1u_4 \\ u_2^2 & u_3^2 & u_5^2 & 2u_2u_3 & 2u_3u_5 & 2u_2u_5 \\ u_4^2 & u_5^2 & u_6^2 & 2u_4u_5 & 2u_5u_6 & 2u_4u_6 \\ u_1u_2 & u_2u_3 & u_4u_5 & u_1u_3+u_2^2 & u_4u_3+u_2u_5 & u_1u_5+u_2u_4 \\ u_2u_4 & u_3u_5 & u_5u_6 & u_2u_5+u_4u_3 & u_3u_6+u_5^2 & u_2u_6+u_4u_5 \\ u_1u_4 & u_2u_5 & u_4u_6 & u_1u_5+u_2u_4 & u_2u_6+u_4u_5 & u_1u_6+u_4^2 \end{bmatrix}. \tag{4.12}$$

For axially symmetric and $2D$ problems, the matrix $\mathbf{Q}$ is tailored by deleting the appropriate rows and columns. The rows and columns of $\mathbf{Q}$ are ordered as follows: x, y, z, xy, yz, xz.

The fast convergence of the Newton iteration with the tangential matrix $\mathbf{C}^{*ep}$ proves its efficiency in spite of the two preceding assumptions we made in connection with the transformation.

5. Solution of the nonlinear elastoplastic problem

5.1. The total Lagrangian formulation. In the course of elastoplastic deformations, the points of the body assume different elastoplastic states. Some points are in elastic state and the rest are in plastic state. We treat the elastoplastic problem by means of the principle of the virtual work. Referring to the book by Bathe [2] but not entering into details, we write the variational equation

$$\int_{{}^oV} \left[\delta\left(\Delta\tilde{\mathbf{E}}_L^{(i)}\right) : \mathbf{C}^{ep} : \Delta\tilde{\mathbf{E}}_L^{(i)} + \delta\left(\Delta\tilde{\mathbf{E}}_{NL}^{(i)}\right) : \mathbf{P}_n^{II}\right] \mathrm{d}^oV = \\ = \delta W_{n+1} - \int_{{}^oV} \delta\left(\Delta\tilde{\mathbf{E}}_L^{(i)}\right) : \mathbf{P}_n^{II}\, \mathrm{d}^oV\,, \quad (5.1)$$

which expresses the equilibrium and compatibility requirements over the time period from t_n to t_{n+1}. The Green-Lagrange strain tensor at the time t_{n+1} is given by

$$\mathbf{E} = \frac{1}{2}\left[\mathbf{F}_{n+1}^T \cdot \mathbf{F}_{n+1} - \mathbf{1}\right] \quad (5.2)$$

where

$$\mathbf{F}_{n+1} = \frac{\partial\,(\mathbf{X} + \mathbf{u}_{n+1})}{\partial\,\mathbf{X}} = \mathbf{1} + \frac{\partial\,\mathbf{u}_{n+1}}{\partial\,\mathbf{X}} = \mathbf{1} + (\nabla\mathbf{u})_{n+1} \equiv 1 + grad\,(\mathbf{u}_{n+1})\,. \quad (5.3)$$

$\mathbf{E}_{n+1}$ can be expressed in terms of the displacement vector as well:

$$\mathbf{E}_{n+1} = \frac{1}{2}\left[(\nabla\mathbf{u})^T + (\nabla\mathbf{u}) + (\nabla\mathbf{u})^T \cdot (\nabla\mathbf{u})\right]_{n+1}\,. \quad (5.4)$$

If convergency is achieved in the i^{th} iteration step by performing a load step from time t_n to t_{n+1}, then it is expedient to decompose the displacement as follows

$$\mathbf{u}_{n+1}^{(i)} = \mathbf{u}_n + \tilde{\mathbf{u}}^{(i)} = \mathbf{u}_n + \tilde{\mathbf{u}}^{(i-1)} + \tilde{\tilde{\mathbf{u}}}^{(i)} \equiv \mathbf{u}_{n+1}^{(i-1)} + \tilde{\tilde{\mathbf{u}}}^{(\mathbf{i})}\,, \quad (5.5)$$

where $\tilde{\mathbf{u}}^{(i)}$ denotes the displacement increment corresponding to $\Delta\mathbf{u}^{(i)}$. Consequently, equation (5.4) can be rewritten:

$$\mathbf{E}_{n+1}^{(i)} = \mathbf{E}_n + \Delta\tilde{\mathbf{E}}_L^{(i)} + \Delta\tilde{\mathbf{E}}_{NL}^{(i)}\,, \quad (5.6)$$

where

$$\Delta\tilde{\mathbf{E}}_L^{(i)} = \frac{1}{2}\left[\left(\nabla\tilde{\mathbf{u}}^{(i)}\right)^T + \left(\nabla\tilde{\mathbf{u}}^{(i)}\right) + (\nabla\mathbf{u}_n)^T \cdot \left(\nabla\tilde{\mathbf{u}}^{(i)}\right) + \left(\nabla\tilde{\mathbf{u}}^{(i)}\right)^T \cdot (\nabla\mathbf{u}_n)\right] \quad (5.7)$$

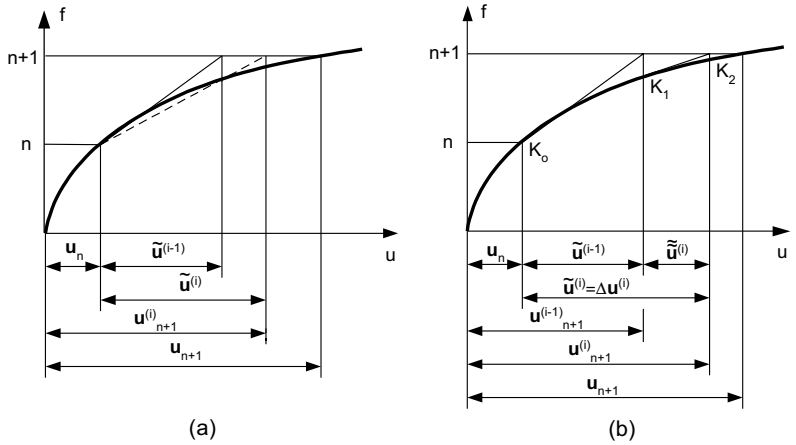

Figure 1. Iteration schemes for one load step

and

$$\Delta\tilde{\mathbf{E}}^{(i)}_{NL} = \frac{1}{2}\left[\left(\nabla\tilde{\mathbf{u}}^{(i)}\right)^T \cdot \left(\nabla\tilde{\mathbf{u}}^{(i)}\right)\right]. \tag{5.8}$$

It is more favorable to recalculate the constitutive matrix $\mathbf{C}^{ep}$ in each iteration step (see Figure 6.1b) than to follow the iteration scheme shown in Figure 6.1a. Therefore equation (5.1) is modified as

$$\int_{{}^oV}\left[\delta\left(\Delta\overset{\approx}{\mathbf{E}}{}^{(i)}_L\right) : \mathbf{C}^{ep}_{(i-1)} : \Delta\overset{\approx}{\mathbf{E}}{}^{(i)}_L + \delta\left(\Delta\overset{\approx}{\mathbf{E}}{}^{(i)}_{NL}\right) : \mathbf{P}^{II}_n\right] \mathrm{d}^oV =$$

$$= \delta W_{n+1} - \int_{{}^oV}\delta\left(\Delta\overset{\approx}{\mathbf{E}}{}^{(i)}_L\right) : \mathbf{P}^{II(i-1)}_{n+1}\,\mathrm{d}^oV, \tag{5.9}$$

where

$$\mathbf{E}^{(i)}_{n+1} = \mathbf{E}^{(i-1)}_{n+1} + \Delta\overset{\approx}{\mathbf{E}}{}^{(i)}_L + \Delta\overset{\approx}{\mathbf{E}}{}^{(i)}_{NL}. \tag{5.10}$$

$$\Delta\overset{\approx}{\mathbf{E}}{}^{(i)}_L = \frac{1}{2}\left[\left(\nabla\overset{\approx}{\mathbf{u}}{}^{(i)}\right)^T + \left(\nabla\overset{\approx}{\mathbf{u}}{}^{(i)}\right) + \left(\nabla\mathbf{u}^{(i-1)}_{n+1}\right)^T \cdot \left(\nabla\overset{\approx}{\mathbf{u}}{}^{(i)}\right) + \left(\nabla\overset{\approx}{\mathbf{u}}{}^{(i)}\right)^T \cdot \left(\nabla\mathbf{u}^{(i-1)}_{n+1}\right)\right] \tag{5.11}$$

$$\Delta\overset{\approx}{\mathbf{E}}{}^{(i)}_{NL} = \frac{1}{2}\left[\left(\nabla\overset{\approx}{\mathbf{u}}{}^{(i)}\right)^T \cdot \left(\nabla\overset{\approx}{\mathbf{u}}{}^{(i)}\right)\right] \tag{5.12}$$

$$\mathbf{P}^{II(i-1)}_{n+1} = J^{(i-1)}_{n+1}\left(\mathbf{U}^{(i-1)}_{n+1}\right) \cdot \mathbf{t}^{(i-1)}_{n+1} \cdot \left(\mathbf{U}^{(i-1)}_{n+1}\right)^{-1} \tag{5.13}$$

5.2. Finite element discretization. For the numerical treatment of (5.9), we perform the discretization by the finite element method. The increment in displacement is approximated as

$$\overset{\approx}{\mathbf{u}}{}^{(i)} \quad \Longrightarrow \quad \mathbf{N}(\mathbf{X})\,\overset{\approx}{\mathbf{q}}{}^{(i)} \tag{5.14}$$

where $\mathbf{N}(\mathbf{X})$ is the matrix of shape functions, $\overset{\approx}{\mathbf{q}}^{(i)}$ is the vector of displacement parameters. The matrix of shape functions can be constructed by using either the product space or the truncated space [18].

Using the approximation (5.14), we can give the vector of the strain increments corresponding to the Green-Lagrange strain tensor

$$\Delta\overset{\approx}{\mathbf{E}}^{(i)} \Longrightarrow \overset{\approx}{\boldsymbol{\varepsilon}}_L^{(i)} + \overset{\approx}{\boldsymbol{\varepsilon}}_{NL}^{(i)} = \mathbf{B}_L^{(i-1)}(\mathbf{X})\,\overset{\approx}{\mathbf{q}}^{(i)} + \mathbf{B}_{NL}^{(i-1)}(\mathbf{X})\,\overset{\approx}{\mathbf{q}}^{(i)} \tag{5.15}$$

where $\overset{\approx}{\boldsymbol{\varepsilon}}_L^{(i)}$ and $\overset{\approx}{\boldsymbol{\varepsilon}}_{NL}^{(i)}$ are the so-called linear and nonlinear strain increments, respectively.

Making use of equations (5.14) and (5.15), we can discretize the integrals below:

$$\int_{{}^oV} \delta\left(\Delta\overset{\approx}{\mathbf{E}}_L^{(i)}\right) : \mathbf{C}_{(i-1)}^{ep} : \Delta\overset{\approx}{\mathbf{E}}_L^{(i)}\,\mathrm{d}^oV \Longrightarrow \delta\overset{\approx}{\mathbf{q}}^{(i)T} \underbrace{\int_{{}^oV} \mathbf{B}_L^{(i-1)T}\mathbf{C}_{(i-1)}^{ep}\mathbf{B}_L^{(i-1)}\mathrm{d}^oV}_{\mathbf{K}_L^{(i-1)}} \overset{\approx}{\mathbf{q}}^{(i)}\ , \tag{5.16}$$

$$\int_{{}^oV} \delta\left(\Delta\overset{\approx}{\mathbf{E}}_{NL}^{(i)}\right) : \mathbf{P}_n^{II}\,\mathrm{d}^oV \Longrightarrow \delta\overset{\approx}{\mathbf{q}}^{(i)T} \underbrace{\int_{{}^oV} \mathbf{B}_{NL}^{(i-1)T}\,\boldsymbol{\sigma}_n\,\mathbf{B}_{NL}^{(i-1)}\mathrm{d}^oV}_{\mathbf{K}_{NL}^{(i-1)}} \overset{\approx}{\mathbf{q}}^{(i)}\ , \tag{5.17}$$

$$\int_{{}^oV} \delta\left(\Delta\overset{\approx}{\mathbf{E}}_L^{(i)}\right) : \mathbf{P}_{n+1}^{II(i-1)}\,\mathrm{d}^oV \Longrightarrow \delta\overset{\approx}{\mathbf{q}}^{(i)T} \underbrace{\int_{{}^oV} \mathbf{B}_L^{(i-1)T}\,\hat{\boldsymbol{\sigma}}_n^{(i-1)}\,\mathrm{d}^oV}_{\mathbf{f}_\sigma^{(i-1)}}\ , \tag{5.18}$$

$$\delta W_{n+1} = \delta\overset{\approx}{\mathbf{q}}^{(i)T}\left[\int_{{}^oV} \mathbf{N}^{To}\,(\rho\mathbf{k})_{n+1}\ \mathrm{d}^oV - \int_{{}^oA_p} \mathbf{N}^{To}\overline{\mathbf{p}}_{n+1}\,\mathrm{d}^oA\right] = \delta\overset{\approx}{\mathbf{q}}^{(i)T}\mathbf{f}_{n+1}\ . \tag{5.19}$$

The load vectors evaluated over the volume ${}^oV$ and the surface ${}^oA_p$ correspond to the reference configuration. Consequently, the traction $\bar{\mathbf{p}}_{n+1}$ exerted at time t_{n+1} can be transformed into the reference configuration

$${}^o\bar{\mathbf{p}}_{n+1} = \mathbf{F}_{n+1}^{-1}\cdot\bar{\mathbf{p}}_{n+1}\,. \tag{5.20}$$

However, the body force follows the transformation rule

$${}^o(\rho\mathbf{k})_{n+1} = (\det\mathbf{J})^{-1}\,(\rho\mathbf{k})_{n+1}\ . \tag{5.21}$$

With the integrals (5.16)-(5.19) and the transformations (5.20), (5.21), the incremental form of the virtual work is discretized as

$$\delta\overset{\approx}{\mathbf{q}}^{(i)T}\left\{[\mathbf{K}_L^{(i-1)}+\mathbf{K}_{NL}^{(i-1)}]\overset{\approx}{\mathbf{q}}^{(i)} - \left(\mathbf{f}_{n+1}-\mathbf{f}_\sigma^{(i-1)}\right)\right\} = 0 \qquad i = 1,2,\ldots \tag{5.22}$$

where $\delta\overset{\approx}{\mathbf{q}}^{(i)T}$ is arbitrary, consequently the following equation holds

$$[\mathbf{K}_L^{(i-1)}+\mathbf{K}_{NL}^{(i-1)}]\overset{\approx}{\mathbf{q}}^{(i)} = \mathbf{f}_{n+1}-\mathbf{f}_{\sigma}^{(i-1)} \equiv \mathbf{r}^{(i-1)} \tag{5.23}$$

in which the sum in brackets is the tangential stiffness matrix:

$$\mathbf{K}_L^{(i-1)}+\mathbf{K}_{NL}^{(i-1)} = \mathbf{K}_T^{(i-1)} \tag{5.24}$$

At the beginning of the iteration ($i = 1$) we use the elastoplastic state obtained at time t_n to initialize the iteration. The iteration is terminated if the unbalanced load vector $\mathbf{r}^{(i)}$ vanishes, i.e., if

$$\left\|\mathbf{r}^{(i)}\right\| = \sqrt{\mathbf{r}^{(i)T}\mathbf{r}^{(i)}} \leq TOL\,\|\mathbf{f}_{n+1}\| \tag{5.25}$$

where $TOL = 0.001 - 0.0001$.

5.3. Updating the stress state. The solution of equation (5.23) in the i^{th} iteration gives the vector of displacements $\overset{\approx}{\mathbf{q}}^{(i)}$, in this way we can calculate $\overset{\approx}{\mathbf{u}}^{(i)}$ from (5.14) and $\mathbf{u}_{n+1}^{(i)}$ from (5.5). Then we obtain the actual stress state as given subsequently.

The time integration of the velocity is performed by the method proposed by Pinsky, Ortiz and Pister [13]. This is a mid-increment scheme, second order accurate and unconditionally stable. The procedure determines the displacement at the middle of the time interval

$$\mathbf{u}_{n+1/2}^{(i)} = \frac{1}{2}\left(\mathbf{u}_n + \mathbf{u}_{n+1}^{(i)}\right) \tag{5.26}$$

The steps of the algorithm:

Step 1. Determination of the deformation gradient for the states $n + 1/2$ and $n + 1$

$$\mathbf{F}_{n+1}^{(i)} = \frac{\partial\left(\mathbf{X}+\mathbf{u}_{n+1}^{(i)}\right)}{\partial\mathbf{X}}, \quad J_{n+1}^{(i)} = \det\left(\mathbf{F}_{n+1}^{(i)}\right), \quad \mathbf{F}_{n+1/2}^{(i)} = \frac{\partial\left(\mathbf{X}+\mathbf{u}_{n+1/2}^{(i)}\right)}{\partial\mathbf{X}}. \tag{5.27}$$

Step 2. Polar decomposition with the method described in Appendix II:

$$\mathbf{F}_{n+1}^{(i)} = \mathbf{R}_{n+1}^{(i)} \cdot \mathbf{U}_{n+1}^{(i)}, \qquad \mathbf{F}_{n+1/2}^{(i)} = \mathbf{R}_{n+1/2}^{(i)} \cdot \mathbf{U}_{n+1/2}^{(i)}. \tag{5.28}$$

Step 3. Integration of the tensor $\mathbf{L} = \dot{\mathbf{F}} \cdot \mathbf{F}^{-1}$:

Since

$$\mathbf{L} = \frac{\partial\mathbf{v}}{\partial\mathbf{x}} = \frac{\partial\mathbf{v}}{\partial\mathbf{X}} \cdot \mathbf{F}^{-1},$$

we can write

$$\frac{\partial}{\partial\mathbf{x}}\frac{\partial\mathbf{u}}{\partial t} = \frac{\partial}{\partial\mathbf{X}}\frac{\partial\mathbf{u}}{\partial t} \cdot \mathbf{F}^{-1},$$

from which it follows by an integration with respect to time t that

$$\int \frac{\partial}{\partial\mathbf{x}}\frac{\partial\mathbf{u}}{\partial t}\,\mathrm{d}t = \int \frac{\partial}{\partial\mathbf{X}}\frac{\partial\mathbf{u}}{\partial t} \cdot \mathbf{F}^{-1}\,\mathrm{d}t.$$

If the deformation gradient is taken at the middle of the time step we get

$$\int \frac{\partial}{\partial \mathbf{x}} \, \mathrm{d}\mathbf{u} = \int \frac{\partial}{\partial \mathbf{X}} \, \mathrm{d}\mathbf{u} \cdot \mathbf{F}^{-1}_{n+1/2} \, .$$

The deformation gradient is then calculated as follows

$$\frac{\partial \left(\Delta \mathbf{u}^{(i)}\right)}{\partial \mathbf{x}} = \frac{\partial \left(\Delta \mathbf{u}^{(i)}\right)}{\partial \mathbf{X}} \cdot \mathbf{F}^{-1}_{n+1/2} \, ,$$

where $\Delta \mathbf{u}^{(i)}$ is the displacement increment

$$\Delta \mathbf{u}^{(i)} = \tilde{\mathbf{u}}^{(i)} = \mathbf{u}^{(i)}_{n+1} - \mathbf{u}_n \, .$$

For the increment of $\mathbf{L}$ we now can write

$$\Delta \mathbf{L}^{(i)} = \Delta \mathbf{F}^{(i)} \cdot \mathbf{F}^{-1}_{n+1/2} \, , \tag{5.29}$$

where the increment of the deformation gradient $\mathbf{F}$ is

$$\Delta \mathbf{F}^{(i)} = \frac{\partial \left(\Delta \mathbf{u}^{(i)}\right)}{\partial \mathbf{X}} \, . \tag{5.30}$$

Step 4. Computation of the symmetric part of $\Delta \mathbf{L}^{(i)}$:

$$\Delta \mathbf{D}^{(i)} = \frac{1}{2} \left[\Delta \mathbf{L}^{(i)} + \Delta \mathbf{L}^{(i)T} \right] \quad . \tag{5.31}$$

Step 5. Transformation of the increment in the rate of deformation tensor to an increment of the unrotated deformation rate tensor:

$$\Delta \mathbf{d}^{(i)} = \mathbf{R}^{(i)T}_{n+1/2} \cdot \Delta \mathbf{D}^{(i)} \cdot \mathbf{R}^{(i)}_{n+1/2} \quad . \tag{5.32}$$

Step 6. With the knowledge of $\Delta \mathbf{d}^{(i)}$ we can perform the calculations detailed in Appendix I in order to determine the elastoplastic state together with the yield surface and the Cauchy stress tensor. Using a symbolic notation

$$\mathbf{t}^{(i)}_{n+1} \Longleftarrow RRA(\mathbf{t}^{(i-1)}_{n+1}, \overline{e}^{p(i-1)}_{n+1}, \boldsymbol{\alpha}^{(i-1)}_{n+1}, \Delta \mathbf{d}^{(i)}) \, , \tag{5.33}$$

where RRA denotes the radial return mapping algorithm.

In the course of the time integration we obtain the following quantities:

the equivalent plastic strain

$$\overline{e}^{p(i)}_{n+1} \, , \tag{5.34}$$

the deviatoric stress at the centre of the yielding surface

$$\boldsymbol{\alpha}^{(i)}_{n+1} \, , \tag{5.35}$$

the deviatoric stress tensor

$$\mathbf{s}^{(i)}_{n+1} \, , \tag{5.36}$$

the total stress tensor

$$\mathbf{t}_{n+1}^{(i)} ,$$

and the elastoplastic consistent matrix $\mathbf{C}_{(i)}^{ep}$ (see (4.11) for details).

Applying the p-version of the finite element method the hydrostatic stress field is smoothed by a low order approximation $(p/2)$.

Step 7. Let us transform the Cauchy stress $\mathbf{t}_{n+1}^{(i)}$ obtained in the unrotated configuration to the reference coordinate system

$$\mathbf{P} = J_{n+1}^{(i)}(\mathbf{U}_{n+1}^{(i)})^{-1} \cdot \mathbf{t}_{\mathbf{n+1}}^{(\mathbf{i})} \cdot (\mathbf{U}_{n+1}^{(i)})^{-1} . \tag{5.37}$$

5.4. The global algorithm of the nonlinear problem. As is given in the previous subsection, we perform the seven steps in each Gauss integration point, and we obtain the point K_1 starting from point K_0 in iteration $i = 1$, then point K_2 from point K_1 in iteration $i = 2$, and so on (see Figure 6.1b). That is, in each iteration i we determine the stiffness matrices $\mathbf{K}_L^{(i-1)}$, $\mathbf{K}_{NL}^{(i-1)}$ and the vector of internal forces $\mathbf{f}_\sigma^{(i-1)}$ with the quantities calculated in the seven steps.

The external forces are applied gradually in a sequence of load steps, and in the course of the equilibrium iteration (i) the elastoplastic condition is always checked.

The scheme of the algorithm:
Loop for the load steps $(n = 1, 2, ..., nload)$.

α. Equilibrium iteration $(i = 1, 2, ...)$.

A/ Generate the system matrices and vectors:

$$\mathbf{K}_L^{(i-1)}, \mathbf{K}_{NL}^{(i-1)}, \mathbf{f}_\sigma^{(i-1)}, \mathbf{f}_\sigma^{(0)} = \mathbf{0} .$$

B/ Solve for $\overset{\approx}{\mathbf{q}}^{(i)}$

$$[\mathbf{K}_L^{(i-1)} + \mathbf{K}_{NL}^{(i-1)}]\overset{\approx}{\mathbf{q}}^{(i)} = \mathbf{f}_{n+1} - \mathbf{f}_\sigma^{(i-1)} \equiv \mathbf{r}^{(i-1)} .$$

C/ Update the vector of displacement parameters

$$\mathbf{q}_{n+1}^{(i)} = \mathbf{q}_{n+1}^{(i-1)} + \overset{\approx}{\mathbf{q}}^{(i)} .$$

D/ Loop for the finite elements $(e = 1, ..., n_e)$:
a/ Loop for the Gauss integration points:
I/ Determination of the displacement field

$$\mathbf{u}_{n+1}^{(i)} = \mathbf{N}(\mathbf{X})\, \mathbf{q}_{n+1}^{(i)} .$$

II/ Calculate the displacement of the half step

$$\mathbf{u}_{n+1/2}^{(i)} = \frac{1}{2}\left(\mathbf{u}_n^{(i)} + \mathbf{u}_{n+1}^{(i)}\right) .$$

III/ Update the stresses (Step 1-7) in accordance with Section 5.3.
b/ Generate the element stiffness matrices and the vector of internal forces

$$\left(\mathbf{K}_L^{(i)}\right)_e, \left(\mathbf{K}_{NL}^{(i)}\right)_e, \left(\mathbf{f}_\sigma^{(i)}\right)_e .$$

E/ Check for convergence
if $\left\|\mathbf{r}^{(i)}\right\| \leq TOL \left\|\mathbf{f}_{n+1}\right\|$ then go to (β) else $i = i + 1$ and go to (A) .

β. Prepare the next load step $n = n + 1$

$$\mathbf{q}_n \Longleftarrow \mathbf{q}_{n+1}, \qquad \mathbf{f}_n \Longleftarrow \mathbf{P}_n^{II} .$$

If $n \leq nload$ then go to (α) else STOP.

6. Numerical example

An axisymmetric cylinder with a height of 40 mm and a diameter of 35 mm is compressed between two rough rigid plates (see Figure 2). The material is elastioplastic with the following hardening rule

$$(\overline{e}^p) = \sigma_\infty - (\sigma_\infty - \sigma_Y) \exp\left(-\gamma \overline{e}^p\right) + \sigma^o \overline{e}^p$$

where $\sigma_\infty = 0.343$ MPa, $\sigma_Y = 0.243$ MPa, $\sigma^o = 0.15$ MPa, $\gamma = 0.1$. The elastic properties of the material are characterized by Young's modulus and Poisson's ratio: $E = 70$ MPa, $\nu = 0.2$.

Two meshes were used for the discretization of the quarter of the domain. In the first mesh denoted by (2×2) there are 4 axsisymmetric p-extension elements [18], the mesh has two elements in the radial direction and two elements in axial direction. The second mesh denoted by (4×4) has a double density compared to the first one, i.e., it has direction and four elements in the axial direction. First we will use the product space for the approximation of the displacement fields. We note that the number of bubble functions of the truncated space is equal to 15 for $p = 8$, however we have 49 bubble functions in the product space for $p = 8$. This gives a possibility to investigate different ways in which the approximation of the volumetric change. Symmetry conditions are specified on the axis and in the middle plane of the cylinder. Sticking conditions and a prescribed compressive displacement are specified at the tool-workpiece interface.

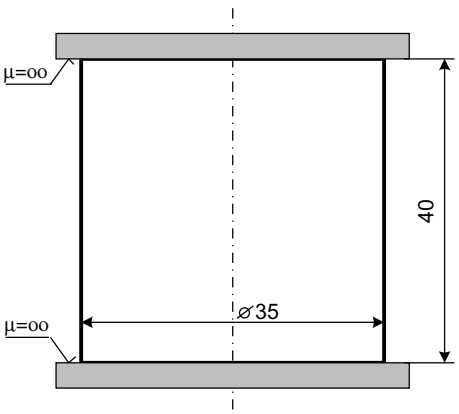

Figure 2.

The total height reduction of 20% is obtained in 10 increments. The polynomial degree of the approximation is $p = 8$, the numerical integration is performed on 9×9 Gauss points. The volumetric change is evaluated directly from the displacement fields.

The deformed shapes and the distributions of the plastic strains $\overline{e}^p$ are displayed for the two meshes in Figures 3 and 4. In the gray scale of plastic strains black corresponds to the maximum value (1.137) and white corresponds to the minimum value (0). The maximum value (1.137) has been computed at the upper right corner of the domain. The corresponding von Mises stresses have also been evaluated as shown in Figures 5 and 6. In the gray scale of the von Mises stresses black corresponds to the maximum value ($0.4015\,MPa$) and white corresponds to the minimum value (0). The results for the different meshes show good agreement. Here we see the effectiveness of the p-extension as the results are reliable also for a coarse mesh.

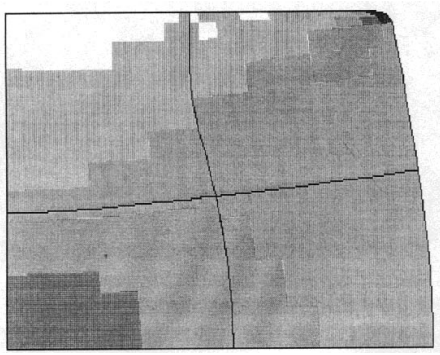

Figure 3.
Distribution of plastic strains for the mesh (2×2)

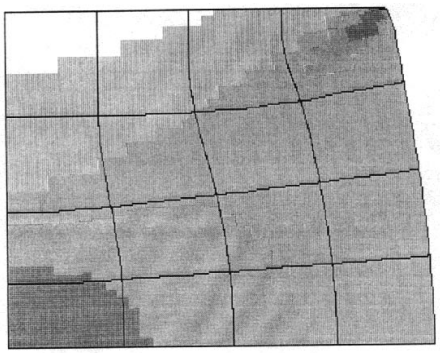

Figure 4.
Distribution of plastic strains for the mesh (4×4)

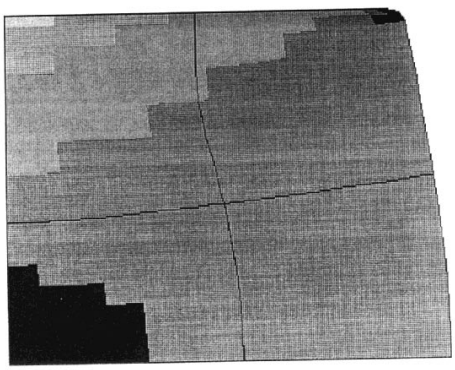

Figure 5.
Distribution of the von Mises stress for the mesh (2×2)

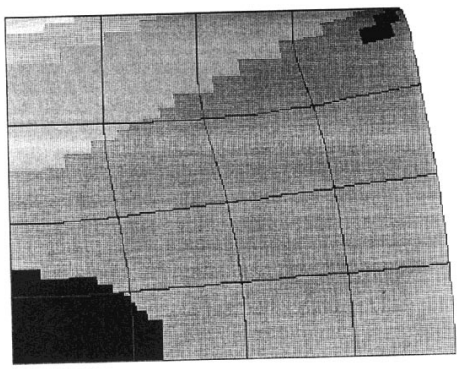

Figure 6.
Distribution of the von Mises stress for the mesh (2×2)

The weakening of the volumetric change is not needed for the product space if $p = 8$ and the order of integration is 9×9. In this case, the number of integration points for one element (81) is smaller than the number of bubble functions (98), therefore the element has extra degrees of freedom to satisfy the elastoplastic equations.

The truncated space [18] can also be used for the solution of the elastoplastic problem. We experienced that the volumetric change should be weakened. Therefore we applied the least square method with a polynomial degree of $p/2$ to smooth the volumetric change field. The same layout of the problem has been analyzed with the following material parameters: $\sigma_\infty = 30\,\mathrm{MPa}$, $\sigma_Y = 20\,\mathrm{MPa}$, $\sigma^o = 2\,\mathrm{MPa}$, $\gamma = 0.1$. The elastic properties are given by the Young's modulus $E = 2700\,\mathrm{MPa}$, and the Poisson's ratio $\nu = 0.35$. The total height reduction, which is 10%, is obtained in 5 increments.

For the second mesh (4×4) we performed the computations for different degrees of approximation by using the truncated space. The computed characteristic stress components are shown in Table 1. As can be seen, we obtained similar results for $p = 6$ and $p = 8$, i.e., convergence has been achieved by the p-version of the finite element method for a large strain elastoplastic problem.

Table 1. Characteristic stress values

p	min/max	σ_r	σ_φ	σ_z	τ_{rz}
2	min	$-0.2745 \cdot 10^2$	$-0.2797 \cdot 10^2$	$-0.4076 \cdot 10^2$	$-0.1042 \cdot 10^2$
2	max	$+0.1604 \cdot 10^2$	$+0.1155 \cdot 10^2$	$-0.3289 \cdot 10^1$	$+0.5686 \cdot 10^1$
4	min	$-0.4093 \cdot 10^2$	$-0.4094 \cdot 10^2$	$-0.6099 \cdot 10^2$	$-0.9211 \cdot 10^1$
4	max	$+0.1123 \cdot 10^2$	$+0.1121 \cdot 10^2$	$-0.8859 \cdot 10^1$	$+0.6156 \cdot 10^1$
6	min	$-0.2970 \cdot 10^2$	$-0.3262 \cdot 10^2$	$-04746 \cdot 10^2$	$-0.8916 \cdot 10^1$
6	max	$+0.6110 \cdot 10^1$	$+0.9757 \cdot 10^1$	$-0.1119 \cdot 10^2$	$+0.5541 \cdot 10^1$
8	min	$-0.3086 \cdot 10^1$	$-0.3204 \cdot 10^2$	$-0.4609 \cdot 10^2$	$-0.8887 \cdot 10^1$
8	max	$+0.6110 \cdot 10^1$	$+0.9766 \cdot 10^2$	$-0.1118 \cdot 10^2$	$0.6324 \cdot 10^1$

We note that when the height reduction was increased over 20%, the element in the upper right corner of the mesh became distorted so the convexity of the element was destroyed.

7. Conclusion

A finite element code has been developed to solve large strain elastoplastic problems using p-extension elements. The total Lagrangian formulation of the finite element method has been implemented. Large and incompressible plastic deformations were assumed. The constitutive computations have been performed in the unrotated frame. The radial return mapping algorithm was used for the treatment of the yield surface. Kinematic and isotropic hardening rules were adopted.

From the numerical experiments we concluded that p-extension of the finite elements can be applied for the analysis of large strain elastoplastic problems. The

approximation of the displacement fields has been investigated by means of two different polinomial spaces: the product space and the trunceted space.

Making use of the product space and integrating numerically with a (9×9) integration order, we obtained smooth solutions for the case when p was equal to 8 both for the displacement fields and for the volumetric change. The advantageous behavior of the product space follows from the fact that the number of bubble functions is greater than the number of integration points.

Applying the truncated space with polynomial degree p for the approximation of the displacement fields, we obtained smooth solutions if the volumetric change was weakened. We experienced that smoothing the volumetric change by the least square method with polynomials of degree $p/2$ provides a proper choice for the different values of p (for $p = 2, 4, 6, 8$).

Since the p-extension of the finite elements are sensitive for stress concentrations, the deformed elements may be distorted at the vicinity of the singular points. Therefore remeshing of the domain is required even for relatively small displacements.

8. Appendix I: Radial return mapping

We shall assume that all quantities are known at time t_n. Increasing the load gradually we determine all quantities with an elastic prediction. Therefore the point representing the elastic state we have predicted will be, in all probability, outside the yield surface. Then due to an orthogonal mapping the point will be placed on the surface. The elastic prediction gives the stress deviatoric tensor:

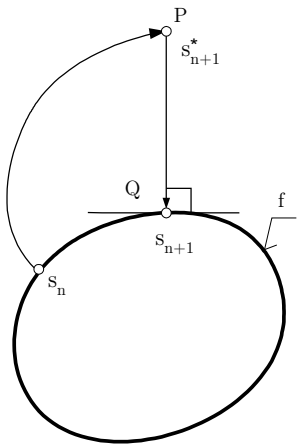

Figure 7.

$$\mathbf{s}^*_{n+1} = \mathbf{s}_n + 2G\Delta\mathbf{e}_{n+1}\,. \tag{8.1}$$

The treatment of the plastic problem is practically an optimization problem. Let f be an arbitrary but convex yield surface. We have to find the point of f with the smallest distance from a point elastically predicted and located outside f. The unit normal to the yield surface at the end of the time interval $[t_n, t_{n+1}]$ is denoted by $\mathbf{n}$. It is obvious that

$$\hat{\mathbf{n}} = \frac{\partial f}{\partial \boldsymbol{\xi}}\bigg|_{n+1} \cdot \frac{1}{\left\|\frac{\partial f}{\partial \boldsymbol{\xi}}\right\|_{n+1}} = \frac{\boldsymbol{\xi}_{n+1}}{\left\|\frac{\partial f}{\partial \boldsymbol{\xi}}\right\|_{n+1}}\,. \tag{8.2}$$

Making use of equation (3.7) we can write

$$\frac{\partial f}{\partial \boldsymbol{\xi}} = \frac{\partial}{\partial \boldsymbol{\xi}}\sqrt{\boldsymbol{\xi} : \boldsymbol{\xi}} = \frac{\boldsymbol{\xi}}{\|\boldsymbol{\xi}\|}\,,$$

where

$$\boldsymbol{\xi} = \mathbf{s}_{n+1} - \boldsymbol{\alpha}_{n+1} \quad . \tag{8.3}$$

Starting from the elastoplastic state corresponding to t_n one can obtain the state at t_{n+1} through the following integral

$$\int_{t_n}^{t_{n+1}} 2G\dot{\mathbf{e}}^p d\tau = \int_{t_n}^{t_{n+1}} 2G\gamma\hat{\mathbf{n}}\, d\tau,$$

which is calculated approximately as

$$2G\left(\gamma\Delta t\right)\,\hat{\mathbf{n}}\ ,$$

where Δt is the time step ($\Delta t = t_{n+1} - t_n$). Therefore

$$\mathbf{s}_{n+1} = \mathbf{s}^*_{n+1} - 2G\left(\gamma\Delta t\right)\,\hat{\mathbf{n}}\,. \tag{8.4}$$

Since the yield surface is modified due to hardening, we need to calculate the equivalent strain as well

$$\bar{e}^p_{n+1} = \bar{e}^p_n + \int_{t_n}^{t_{n+1}} \sqrt{\frac{2}{3}}\left\|\dot{\mathbf{e}}^p\right\|\, d\tau = \bar{e}^p_n + \sqrt{\frac{2}{3}}\left(\gamma\Delta t\right) \quad . \tag{8.5}$$

Making use of equation (3.17), we can write

$$\begin{aligned}\boldsymbol{\alpha}_{n+1} &= \boldsymbol{\alpha}_n + \int_{t_n}^{t_{n+1}} \frac{2}{3}H'_\alpha\left(\bar{e}^p\right)\,\gamma\hat{\mathbf{n}}\, d\tau = \boldsymbol{\alpha}_n + \tfrac{2}{3}H'_\alpha\left(\bar{e}^p_{n+1/2}\right)\left(\gamma\Delta t\right)\,\hat{\mathbf{n}} \\ &= \boldsymbol{\alpha}_n + \frac{2}{3}\frac{H_\alpha\left(\bar{e}^p_{n+1}\right) - H_\alpha\left(\bar{e}^p_n\right)}{\bar{e}^p_{n+1} - \bar{e}^p_n}\left(\gamma\Delta t\right)\,\hat{\mathbf{n}}\end{aligned}$$

for the translation of the centre of the yield surface. Taking (8.5) into account and introducing the notation

$$\Delta H_\alpha = H_\alpha\left(\bar{e}^p_{n+1}\right) - H_\alpha\left(\bar{e}^p_n\right)$$

we have

$$\boldsymbol{\alpha}_{n+1} = \boldsymbol{\alpha}_n + \sqrt{\frac{2}{3}}\Delta H_\alpha\,\hat{\mathbf{n}}\,. \tag{8.6}$$

From (8.3), (8.4) and (8.6) the value of $\boldsymbol{\xi}$ at time t_{n+1} is written as

$$\boldsymbol{\xi}_{n+1} = \mathbf{s}_{n+1} - \boldsymbol{\alpha}_{n+1} = \mathbf{s}^*_{n+1} - \boldsymbol{\alpha}_n - \left[2G\left(\gamma\Delta t\right) + \sqrt{\frac{2}{3}}\Delta H_\alpha\right]\,\hat{\mathbf{n}} \quad . \tag{8.7}$$

Substituting the tensor

$$\boldsymbol{\xi}^*_{n+1} = \mathbf{s}^*_{n+1} - \boldsymbol{\alpha}_n\,, \tag{8.8}$$

we can determine the normal vector $\hat{\mathbf{n}}$

$$\hat{\mathbf{n}} = \frac{\boldsymbol{\xi}^*_{n+1}}{\left\|\boldsymbol{\xi}^*_{n+1}\right\|}\,. \tag{8.9}$$

From (3.7), (8.7) and (8.9) a nonlinear equation is obtained

$$\begin{aligned} f = f(\gamma\Delta t) &= -\sqrt{\tfrac{2}{3}}\ \ \left(\bar{e}^p_{n+1}\right) + \left\| \boldsymbol{\xi}^*_{n+1} - \left[2G\left(\gamma\Delta t\right) + \sqrt{\tfrac{2}{3}}\Delta H_\alpha\right] \tfrac{\boldsymbol{\xi}^*_{n+1}}{\|\boldsymbol{\xi}^*_{n+1}\|} \right\| \\ &= -\sqrt{\tfrac{2}{3}}\ \ \left(\bar{e}^p_{n+1}\right) + \left\|\boldsymbol{\xi}^*_{n+1}\right\| - \left[2G\left(\gamma\Delta t\right) + \sqrt{\tfrac{2}{3}}\Delta H_\alpha\right] = 0\,, \end{aligned} \tag{8.10}$$

where

$$\bar{e}^p_{n+1} = \bar{e}^p_n + \sqrt{\frac{2}{3}}\left(\gamma\Delta t\right) \quad ,$$

and the functions $\left(\bar{e}^p\right), H_\alpha\left(\bar{e}^p\right)$ are also nonlinear. Since all the quantities are known at time t_n, we can determine $(\gamma\Delta t)$. Introducing the notation $\lambda = \gamma\Delta t$, the steps of the Newton iteration are as follows:

$$I \qquad \bar{e}^{p(k)}_{n+1} = \bar{e}^p_n + \sqrt{\frac{2}{3}}\lambda^{(k)}\,,$$

$$II \qquad D\,f\left(\lambda^{(k)}\right) \equiv \frac{\partial f}{\partial \bar{e}^p_{n+1}}\frac{\partial \bar{e}^p_{n+1}}{\partial \lambda} = -2G\left[1 + \frac{{}' + H'_\alpha}{3G}\right]^{(k)} \quad ,$$

$$III \qquad \lambda^{(k+1)} = \lambda^{(k)} - \frac{f\left(\lambda^{(k)}\right)}{D\,f\left(\lambda^{(k)}\right)}\,,$$

$$IV \qquad \text{If } \left|f\left(\lambda^{(k)}\right)\right| \geq \text{TOL then } k \longleftarrow k+1 \text{ and goto(I) else STOP.}$$

Solving the nonlinear equation (8.10), we can calculate $\bar{e}^p_{n+1}$ from (8.5) and $\boldsymbol{\alpha}_{n+1}$ from (8.6). The deviatoric stress tensor $\mathbf{s}_{n+1}$ is determined in such a way that we measure the radius of the yield surface, that is the value

$$\mathbf{s}_{n+1} = \boldsymbol{\alpha}_{n+1} + \sqrt{\frac{2}{3}}\ \ \left(\bar{e}^p_{n+1}\right)\,\hat{\mathbf{n}} \tag{8.11}$$

from the centre of the yield surface in the direction $\hat{\mathbf{n}}$. The elastic part of the stress tensor is calculated from the volume change:

$$\mathbf{t}_{n+1} = \mathbf{s}_{n+1} + K\,\mathrm{tr}(\Delta\boldsymbol{\varepsilon})\,\mathbf{1} = \mathbf{s}_{n+1} + K\,\left(\det\mathbf{F}_{n+1} - 1\right)\,\mathbf{1} \tag{8.12}$$

where

$$\Delta\boldsymbol{\varepsilon} = \boldsymbol{\varepsilon} - \boldsymbol{\varepsilon}_n\,. \tag{8.13}$$

The iteration over the interval $[t_n, t_{n+1}]$ leads to the elastoplastic state to be sought. The quantities in the iteration step i are denoted by $()^{(i)}_{n+1}$.

9. Appendix II: The polar decomposition of F

The steps of the procedure detailed below were proposed by Hager and Carlson [9], Healy and Dodds [7]:

Step 1: Calculate the right Cauchy-Green strain tensor and its second power

$$\mathbf{C} = \mathbf{F}^T \cdot \mathbf{F}, \qquad \mathbf{C}^2 = \mathbf{C}^T \cdot \mathbf{C}\,. \tag{9.1}$$

Step 2: Determine the eigenvalues

$$\lambda_1^2, \lambda_2^2, \lambda_3^2 \tag{9.2}$$

of $\mathbf{C}$ using the Jacobi method [2].

Step 3: Determine the scalar invariants of the tensor $\mathbf{U}$

$$I_U = \lambda_1+\lambda_2+\lambda_3, \quad II_U = \lambda_1\lambda_2+\lambda_2\lambda_3+\lambda_3\lambda_1, \quad III_U = \lambda_1\lambda_2\lambda_3 = \det \mathbf{F} = J\,. \tag{9.3}$$

Step 4: Determine $\mathbf{U}$ and $\mathbf{U}^{-1}$ in terms of the invariants of $\mathbf{C}$, $\mathbf{C}^2$

$$\mathbf{U} = \beta_1 \left(\beta_2 \mathbf{1} + \beta_3 \mathbf{C} - \mathbf{C}^2\right)\,, \tag{9.4}$$

where

$$\beta_1 = \frac{1}{(I_U II_U - III_U)}, \quad \beta_2 = I_U III_U, \quad \beta_3 = I_U^2 - II_U$$

and

$$\mathbf{U}^{-1} = \gamma_1 \left(\gamma_2 \mathbf{1} + \gamma_3 \mathbf{C} + \gamma_4 \mathbf{C}^2\right) \tag{9.5}$$

where

$$\gamma_1 = \frac{1}{III_U \left(I_U II_U - III_U\right)}, \qquad \gamma_2 = I_U II_U^2 - III_U \left(I_U^2 + II_U\right)$$
$$\gamma_3 = -III_U - I_U \left(I_U^2 + 2II_U\right), \quad \gamma_4 = I_U\,.$$

Step 5: Calculation of the tensor $\mathbf{R}$ in the knowledge of $\mathbf{F}$ and $\mathbf{U}^{-1}$

$$\mathbf{R} = \mathbf{F} \cdot \mathbf{U}^{-1} \tag{9.6}$$

Acknowledgement. The support provided by the Hungarian National Research Foundation (project No. T025172) is gratefully acknowledged.

REFERENCES

1. Adkins, J.E., and Rivlin,R.S.: *Large Elastic Deformations of Isotropic Materials*, Part IX. Pl.Trans. 1952.
2. Bathe, K.J.: *Finite Element Procedures*, Prentice-Hall, 1996.
3. Doods, R.H.: *Numerical techniques for plasticity computations in finite-element analysis.* Computer & Structures, **26**, (1987), 767-779.
4. Flanagan, D.P. and Taylor, L.M.: *An accurate numerical algorithm for stress integration with finite rotations*, Comp. Math. Appl. Mech. Eng. **62**, (1987), 305-320.
5. Hallquist, J.O.: *NIKE 2D-A Vectorized, Implicit Finite Deformation, Finite-Element Code for Analysing the Static and Dynamic Response of 2D Solids*, Lawrence Livermore Laboratory Internal Report, UCID-19677, 1983.

6. Hallquist, J.O.: *NIKE 3D-A Vectorized, Implicit Finite Deformation, Finite-Element Code for Analysing the Static and Dynamic Response of 3D Solids*, Lawrence Livermore Laboratory Internal Report, UCID-18822, 1983.
7. Healy,B.E. and Dodds, R.H.: *A large strain plasticity model for implicit finite element analyses*, Computational Mechanics, **9**, (1992), 95-112.
8. Hill, R.: *Aspects of invariance in solid mechanics*, Adv. In Appl. Mech. **18**, (1978), 1-75.
9. Hoger, A. and Carlson, D.E.: *Determination of the strech and rotation in the polar decomposition of the deformation gradient*, Quart. Appl. Math. **10**. (1984), 113-117.
10. Kozák, I.: *Relative Motion of Continua and Time Derivatives of Tensors*, Department of Mechanics, University of Miskolc, Miskolc, 1995.
11. Lee, E.H.: *Elastic-plastic deformation at finite strain,* J. Appl. Mech. **36**, (1969), 1-6.
12. Ogden, R.W.: *Non-linear Elastic Deformations*, Ellis Horwood, Chichester, 1984.
13. Pinsky, P.M., Ortiz, M. and Pister, K.S.: *Numerical integration of rate constitutive equations in finite deformation analysis*, Comp. Math. Appl. Mech. Eng. **40**, (1983), 137-158.
14. Reed, K.W. and Atluri, S.N.: *Constitutive modeling and computational implementation for finite strain plasticity*, Int. J. Plasticity, **1**, (1985), 63-87.
15. Simo, J.C. and Ortiz,M.: *A unified approach to finite deformation elasto-plastic analysis based on the use of hyper-elastic constitutive equations,* Comp. Math. Appl. Mech. Eng. **49**, (1985), 221-245.
16. Simo, J.C. and Taylor, R.S.: *Consistent tangent operations for rate-independent elastoplasticity*, Comp. Math. Appl. Mech. Eng. **48**, (1985), 101-118.
17. Simo, J.C. and Taylor, R.S.: *A return mapping algorithm for plane stress elastoplasticity.* Int. J. Num. Meth. Engng. **22**, (1986), 649-670.
18. Szabó, B.A. and Babuska, I.: *Finite Element Analysis*, Wiley-Interscience Publications, 1991.